Nerve growth factor causes epinephrine release dysfunction by regulating phenotype alterations and the function of adrenal medullary chromaffin cells in mice with allergic rhinitis

CHAO LIU[1,2*], JIAN-PING LIANG[1*], XIAO-LIN HUANG[3], ZHONG LIU[1], AN-BING ZHANG[1], NIAN-GEN DENG[4], ZI-FENG WEI[2] and JUN WANG[2]

[1]Department of Respiratory Disease, Zhongshan People's Hospital, Zhongshan, Guangdong 528403; [2]The Second Department of Respiratory Disease, Jiangxi Provincial People's Hospital, The First Affiliated Hospital of Nanchang Medical College, Nanchang, Jiangxi 330006; [3]Dental Implant and Restoration Centre, Zhongshan People's Hospital, Zhongshan, Guangdong 528403; [4]Department of Respiratory Disease, Ji'an First People's Hospital, Ji'an, Jiangxi 343099, P.R. China

Received September 6, 2022; Accepted December 6, 2022

DOI: 10.3892/mmr.2023.12926

Abstract. The presence of allergic rhinitis (AR) is an increased risk factor for the occurrence of bronchial asthma (BA). Nerve growth factor (NGF), in addition to its key role in the development and differentiation of neurons, may also be an important inflammatory factor in AR and BA. However, the pathogenesis of the progression of AR to BA remains to be elucidated. The present study aimed to investigate the ability of NGF to mediate nasobronchial interactions and explore possible underlying molecular mechanisms. In the present study, an AR mouse model was established and histology of nasal mucosa tissue injury was determined. The level of phenylethanolamine N-methyl transferase in adrenal medulla was determined by immunofluorescence. Primary adrenal medullary chromaffin cells (AMCCs) were isolated and cultured from the adrenal medulla of mice. The expression levels of synaptophysin (SYP), STAT1, JAK1, p38 and ERK in NGF-treated and untreated AMCCs were detected by reverse-transcription-quantitative PCR and western blotting. The epinephrine (EPI) and norepinephrine (NE) concentrations were measured by ELISA. It was found that the expression of SYP in AMCCs was enhanced in the presence of NGF, whereas, the concentration of EPI decreased significantly under the same conditions. Furthermore, NGF mediated the phenotypic and functional changes of AMCCs, resulting in decreased EPI secretion via JAK1/STAT1, p38 and ERK signaling. In conclusion, these findings could provide novel evidence for the role of NGF in regulating neuroendocrine mechanisms.

Correspondence to: Dr Jun Wang, The Second Department of Respiratory Disease, Jiangxi Provincial People's Hospital, The First Affiliated Hospital of Nanchang Medical College, 152 Aiguo Road, Donghu, Nanchang, Jiangxi 330006, P.R. China
E-mail: wangjun5087@163.com

*Contributed equally

Key words: nerve growth factor, allergic rhinitis, bronchial asthma, adrenal medulla chromaffin cells, epinephrine

Introduction

Allergic rhinitis (AR) and bronchial asthma (BA) are inflammatory diseases of the upper and lower respiratory tracts, respectively. They have similar pathological characteristics and exhibit airway inflammation and hyperresponsiveness. A previous study demonstrated close connections between AR and BA (1). In the absence of BA, subjects with AR have significant lower airway dysfunction, including histological, physiological and biochemical changes (2,3). Studies have suggested that AR typically precedes the occurrence of BA and could be an independent risk factor for the development of BA (4,5). However, the pathogenesis of AR's development into BA is complex and not entirely understood.

Nerve growth factor (NGF) reportedly participates in regulating neuronal survival, differentiation, neurotransmission and neurite growth (6). NGF also exerts multidirectional effects on the mediation of several pathophysiological processes, including immune responses, inflammatory responses and catecholamine production (7-9). Reportedly, the expressions of NGF, IL-6 and vasoactive intestinal peptide (VIP) increase considerably in the nasal lavage fluids of AR mice compared with control group mice (10). Previous evidence suggests that NGF is persistently and highly expressed in nasal epithelium and submucosal tissues of patients with AR and is mostly localized in inflammatory cells (11,12). The level of serum NGF has equally been shown to markedly increase in subjects with AR following allergen stimulation (13,14). In addition, NGF is allegedly involved in the pathophysiological processes of airway inflammation and hyperresponsiveness in patients with AR (15). NGF mediates inflammation not only in the upper airway but also in the lower airway (12,16). NGF-mediated neurogenic inflammation is increasingly being linked to the

pathogenesis of BA (16). The concentration of NGF has been shown to be significantly enhanced in the serum of patients with BA (17). Increased NGF in the bronchial and alveolar epithelia of asthmatic mice is likewise said to be involved in the formation of airway hyperresponsiveness (18). These findings point to NGF being a possible key inflammatory factor linking AR to BA. Previous studies have shown that K252a is a potent protein kinase inhibitor that blocked NGF-induced neurite outgrowth and protein phosphorylation changes (19,20).

The synthesis and secretion of epinephrine (EPI) have been shown to decrease in patients with BA, resulting in the inability of epinephrine *in vivo* to effectively relieve bronchospasm during an asthma attack (21). EPI is synthesized by adrenal medulla chromaffin cells (AMCCs) and then released into the circulatory system. In addition to their endocrine function, AMCCs and nerve cells have the same origin and may also have the potential to transform into nerve cells (22,23). This feature of AMCCs is called redundancy in biology (24). There is evidence that asthmatic pregnancy promotes the differentiation of AMCCs into sympathetic nerve cells in offspring rats, inhibits the synthesis of EPI and causes the dysfunction of bronchodilation (25). An *in vitro* study demonstrated that primary cultured AMCCs transform into neural cell phenotypes following stimulation by exogenous NGF. However, glucocorticoids obstruct this NGF-induced phenotypic transformation of AMCCs (26).

Previous studies reported the presence of an EPI secretion disorder in asthmatic model rats, with a mechanism closely associated with NGF-induced neuronal transformation and endocrine dysfunction in AMCCs (21,27). The present study hypothesized that NGF increased significantly in an AR mouse model and assessed its ability to induce the transformation of AMCCs from endocrine phenotypes to neuronal cell phenotypes and then cause a decrease in EPI secretion. The present study also sought to elucidate the potential underlying molecular mechanisms of the evolution of AR into BA.

Materials and methods

Animals. A total of 40 eight-week-old male C57BL6 mice (22±2 g) was obtained from Hunan SJA Laboratory Animal Co., Ltd. and acclimated to their novel environment for a week before experimentation. The rodents were raised in a pathogen-free environment and fed *ad libitum*. The study protocol used was approved by the Animal Care Committee of Jiangxi Provincial People's Hospital (protocol: 2022-008).

Cells, reagents and antibodies. AMCCs were obtained from the adrenal glands of mice. The ovalbumin (OVA; cat. no. SLBK6455V) was purchased from MilliporeSigma, Aluminum hydroxide [$Al(OH)_3$; cat. no. 20150417] was from Tianjin Damao Chemical Reagent Factory, the Opti-MEM I Reduced Serum Medium (cat. no. 31985070), Dulbecco's Modified Eagle Medium (DMEM; cat. no. 10565016) and Lipofectamine® 3000 (cat. no. L3000150) were from Thermo Fisher Scientific, Inc. Giemsa's stain (cat. no. KGA228) and hematoxylin stain (cat. no. KGA223) were from KeyGen Biotech Co., Ltd. Eosin stain (cat. no. AR1180-2) was from Boster Biological Technology Co., Ltd. BCA Protein Quantitative kit (cat. no. CW0014S), DAB kit (cat. no. CW0125M), TRIzon reagent (cat. no. CW0580S), HiFiScript cDNA Synthesis kit (cat. no. CW2569M), Ultrapure RNA kit (cat. no. CW0581M) and UltraSYBR Mixture (cat. no. CW0957M) were obtained from CoWin Biotechnology Co., Ltd. Polyvinylidene difluoride (PVDF) membranes (cat. no. IPVH00010) were from MilliporeSigma, bovine serum albumin (BSA; cat. no. A8020) and enhanced chemiluminescent solution (ECL; cat. no. PE0010) were from Beijing Solarbio Science & Technology Co., Ltd. Non-fat milk powder (cat. no. P1622) was from Applygen Technology Co., Ltd. The recombinant mouse NGF (cat. no. 50385-MNAC) was purchased from Sino Biological Co., Ltd, K252a (cat. no. 11338) was from Neo Bioscience, Inc. and Mouse Norepinephrine (NE; cat. no. ml063805) and Mouse Epinephrine (EPI) ELISA kits (cat. no. ml002049) from Mlbio (Shanghai Enzyme-linked Biotechnology Co., Ltd.). Primary antibodies against synaptophysin (SYP; cat. no. ab 32127), phenylethanolamine N-methyl transferase (PNMT; cat. no. ab167427) were procured from Abcam. NGF (cat. no. bsm-10806m) and tropomyosin receptor kinase (Trk) A (cat. no. bs-10210R) were purchased from BIOSS. GAPDH (cat. no. TA-08), HRP-conjugated goat-anti-rabbit IgG secondary antibody (cat. no. ZB-2301) and HRP-conjugated goat-anti-mouse IgG secondary antibody (cat. no. ZB-2305) were from OriGene Technologies, Inc. and Cy3-conjugated Goat Anti-Rabbit IgG secondary antibody (cat. no. CW0159) was from CoWin Biotechnology Co., Ltd.

Animal model. During the present study, the mice were kept in a 12-h light/dark cycle room with a temperature of 22±2˚C and humidity of 40-70% and allowed food and water freely. They were randomly divided into four groups after 7 days of adaptive feeding: control group (n=10), Model group (OVA group, n=10), Model + NGF group (n=10) and Model + K252a group (n=10).

To establish the AR model, 50 μg ovalbumin (OVA; MilliporeSigma) and 5 mg $Al(OH)_3$ were precipitated at a 1:1 ratio in 1 ml of saline. The mice were immunized by intraperitoneally injecting them with 1 ml of OVA-$Al(OH)_3$ suspension every other day for eight consecutive spells. On the 15th day, 20 μl of saline containing 5% OVA was administered into both airways of the nasal cavity daily for one week. Mice in the control group received the same treatment but were given saline instead of the OVA solution. Prior to the intranasal challenge, mice in the Model + NGF group were intraperitoneally injected with 8 ng/kg of a 1 ng/ml NGF solution. The Model + K252a group mice received 20 μg/kg of a 2 μg/ml K252a solution (an inhibitor of NGF receptor) via intraperitoneal injections prior to the intranasal challenge. During the study, three mice were sacrificed due to reduced food intake and weight loss. Finally, valid data was obtained from a total of 37 mice. On day 22, blood samples were collected via cardiac puncture (2 ml per mouse) and adrenal glands were immediately removed under aseptic conditions. The mice were anesthetized with sodium pentobarbital (70 mg/kg) via intraperitoneal injection and then sacrificed through vertebral dislocation; death was confirmed when the animals developed cardiac arrest, respiratory arrest and corneal reflex arrest. All procedures were conducted strictly in accordance with the National Institutes of Health Guide for the Care and Use of Laboratory Animals (28). The experimental protocol is presented in Fig. 1.

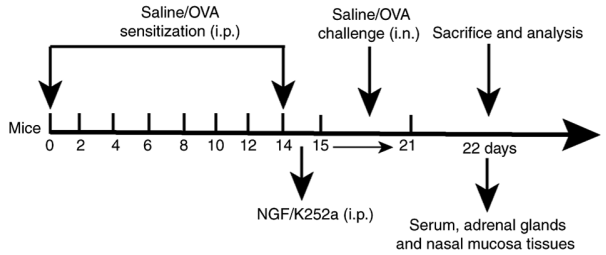

Figure 1. Schematic representation of study protocols. Mice were sensitized to OVA by i.p. injections with OVA-Al(OH)$_3$ suspension every other day for eight consecutive spells and challenged i.n. starting on day 15 with 5% OVA daily for one week. Therapeutic treatment with NGF and K252a (i.p.) before the intranasal challenge. The mice were sacrificed on day 22 by vertebral dislocation and serum samples were collected; adrenal glands were immediately removed under aseptic conditions and nose specimens were obtained for histological analysis. OVA, ovalbumin; i.p., intraperitoneal; i.n., intranasally; NGF, nerve growth factor.

Assessment of Frequencies of Nose Scratching and Sneezing. As previously reported (29), the present study conducted behavioral observations on mice by counting the number of sneezing and nasal rubbing movements for 10 min immediately following the final nasal challenge. Sneezing was characterized by an explosive exhalation followed by a deep inhalation. Nasal rubbing is characterized by scratching around the nose with the animal's forelimbs.

Histopathological analysis of nasal tissues. Nasal mucosa tissues from the mice were fixed in 10 formaldehyde solution at room temperature for 10 days and dehydrated in a graded ethanol series (70, 80, 90 and 99.9%). The transparent tissues were placed in melted paraffin and embedded after the paraffin was completely incorporated into the tissues. Subsequently, the paraffin-embedded nasal mucosa tissues were sectioned into 5 μm and stained with hematoxylin and eosin for 5 min at room temperature. The remaining sections were then deparaffinized in toluene and rehydrated in ethanol with increasing concentrations of water. The endogenous peroxidase was blocked with 3% hydrogen peroxide for 10 min at room temperature. The sections were incubated with polyclonal anti-NGF (1:200) and polyclonal anti-TrkA (1:200) at 4˚C overnight and then incubated with horseradish peroxidase-conjugated secondary antibodies (1:100) at room temperature for 30 min. The sections were developed with DAB at 37˚C for 3 min and then the nuclei were stained with hematoxylin at 37˚C for 3 min. Pathological changes in the nasal mucosa were observed under a light microscope (CX41; Olympus Corporation).

Immunofluorescence staining. The slices of adrenal glands were dewaxed with xylene for 10 min, dehydrated by graded ethanol (100, 100, 95 and 80%) and 0.03% hydrogen peroxide was used to eliminate endogenous peroxidase activity. Antigen-repaired solution was added to repair the antigen of tissues. Following washing with PBS three times for 5 min each time they were permeabilized in 0.5% Triton X-100 at room temperature for 20 min. Non-specific binding was blocked by 5% BSA at room temperature for 30 min and the cells were incubated with anti-phenylethanolamine N-methyl transferase (PNMT; 1:100) at 4˚C overnight, followed by incubation with the Cy3-conjugated Goat Anti-Rabbit IgG (1:200) secondary antibody at room temperature for 30 min. Following washed with PBS three times, nuclei were stained with DAPI for 5 min without light at room temperature and detected with a fluorescence microscope (BX51; Olympus Corporation).

Separation and primary culture of AMCCs. Adrenal glands were immediately collected and washed three times in a cleansing solution containing three antibiotics (100 μg/ml penicillin, 100 μg/ml streptomycin and 50 μg/ml gentamicin) and cut in halves lengthwise and the outer cortex was excised. The medullas were cut into small pieces using sterile curved scissors. Collagenase (0.1%; 45 ml) was then added to the cut pieces and the slices were placed in a 37˚C water bath for 45 min to dissolve. A 5% BSA D-Hanks solution was introduced and the mixture was centrifuged at 250 x g for 5 min at room temperature. The supernatant was removed and a 1% D-Hanks solution was added to the precipitate. A D-Hanks solution containing 5% BSA was poured into another sterile centrifuge tube and the cell suspension was put into the solution. Another centrifugation at 250 x g for 5 min at room temperature yielded cell pellets at the bottom of the tube. Cells were washed with a 1% BSA D-Hanks solution and a 10% FBS-DMEM medium was added. The cells were divided into six groups: Control group, Control + NGF group, Control + K252a group, Model group, Model + NGF group and Model + K252a group. Control and Model group cells were stained with Giemsa at 37˚C for 1-2 min and the results were observed using a light microscope (CX41; Olympus Corporation).

Transmission electron microscopy (TEM). Cells were fixed with 2.5% glutaraldehyde at 37˚C for 3 h, washed with 0.01 M PBS, post-fixed with 1% osmium tetroxide at 37˚C for 1 h, washed with 0.01 M PBS, dehydrated in graded acetone acid, soaked in an epoxy resin embedding medium and 100% acetone at a 1:1 ratio and drenched and embedded in a pure embedding medium. Ultrathin sections of cells (50 nm) were stained with uranyl acetate at 37˚C for 15 min and then lead nitrate at 37˚C for 10 min. Ultrastructural changes were observed using TEM (JEM-1230; JEOL Ltd.).

Cell transfection. For transfection, short hairpin (sh)RNA against STAT1 (sh-STAT1, 5'-GATCCA ACATCTGCCTAGATCGGCTACTGTGAAGCCACAGAT GGGTAGCCGATCTAGGCAGATGTTTTTTTTA-3') and shRNA negative control (sh-NC, 5'-AGCTTAAAAAAAAAC ATCTGCCTAGATCGGCTACCCATCTGTGGCTTCACA GTAGCCGATCTAGGCAGATGTTG-3') were designed and synthesized by Shanghai GenePharma Co., Ltd. Following the manufacturer's instructions, the synthetics were transfected into AMCCs using Lipofectamine® 3000 (Invitrogen; Thermo Fisher Scientific, Inc.). The mass of the plasmids was 2.5 μg. The entire transfection process was carried out in Opti-MEM, a reduced serum medium, at 37˚C for 4 h in a humidified environment containing 5% CO_2. Following transfection, the medium was replaced with a DMEM complete medium containing 20% FBS. Transfection efficiency was detected using reverse-transcription-quantitative polymerase chain reaction (RT-q)PCR and western blotting 48 h post-transfection.

RT-qPCR. Total RNA was extracted from AMCCs using the TRIzon reagent following the manufacturer's instructions. cDNA was synthesized from total RNA using the HiFiScript cDNA Synthesis kit and stored at -70˚C until further use. qPCR was carried out using UltraSYBR Mixture. The thermocycling conditions for PCR were: Initial denaturation for 5 min at 95˚C, followed by 40 cycles of 95˚C for 15 sec and amplification at 60˚C for 1 min. The concentrations of the RT-qPCR products were normalized to GAPDH, which was used as an internal control. The $2^{-\Delta\Delta Cq}$ method was used to calculate the relative mRNA expression (30). The primer sequences are listed in Table I.

Western blot analysis. The AMCCs from different groups were harvested in a RIPA lysis buffer using 1 mM PMSF. Protein concentration was determined using a BCA protein assay kit. Following extraction of total proteins, 30 μg of protein was fractionated on 10% sodium dodecyl sulfate-polyacrylamide gels, electrophoretically transferred onto PVDF membranes, blocked with 5% non-fat milk for 2 h at room temperature, incubated with specific primary antibodies (monoclonal anti-synaptophysin (SYP, 1:1,000), monoclonal anti-p38 (1:1,000), monoclonal anti-STAT1 (1:1,000), polyclonal anti-ERK (1:1,000) and monoclonal anti-JAK1 (1:3,000) at 4˚C overnight and incubated with horseradish peroxidase-conjugated secondary antibodies (1:2,000) at room temperature for 1 h. Fluorescent signals were developed using enhanced chemiluminescent solution. Band densities were analyzed using ImageJ 6.0 software (National Institutes of Health), with the GAPDH protein as an internal reference.

Immunohistochemistry. AMCCs were put in Petri dishes and fixed with 4% paraformaldehyde at room temperature for 15 min, following which 3% hydrogen peroxide was added to remove endogenous peroxidase blocking solution before incubation at room temperature for 10 min. BSA (5%) was added to the Petri dishes dropwise and the content was blocked at 37˚C for 30 min. Next, the cells were exposed to an anti-SYP antibody (Abcam; 1:400) at 4˚C overnight, washed with PBS and incubated with horseradish peroxidase-conjugated secondary antibodies (1:2,000) for 30 min at room temperature. Following another incubation at room temperature without light for 10 min, the signals were detected using 3,3-diaminobenzidine. The cells were then stained with hematoxylin at room temperature for 3 min and examined under a light microscope (CX41; Olympus Corporation).

ELISA. EPI and NE levels were quantified using a commercially available ELISA kit per the manufacturer's recommendations.

Statistical analysis. Each experiment was repeated at least three times. Statistical analyses of all data were conducted using GraphPad Prism 7.0 (GraphPad Software, Inc.). Values were expressed as the mean ± standard deviation. One-way ANOVA, followed by the Tukey post hoc test, was employed for multiple comparisons. $P<0.05$ was considered to indicate a statistically significant difference.

Table I. Primer sequences.

Gene	Primer sequences (5'-3')
SYP	F: CTACTCCTCCTCGGCTGAAT
	R: GCACATAGGCATCTCCTTGATA
JAK1	F: CCAGATTTGTAAGGGGATGGAC
	R: GACCAGACATCAGAGGCGAT
STAT1	F: GTCCCAGAACGGAGGTGAAC
	R: AGTTCGCTTAGGGTCGTCA
p38	F: CCCAGATGCCGAAGATGAACT
	R: TCATAGGTCAGGCTCTTCCACTC
ERK	F: ATCACATCCTGGGTATTCTTGG
	R: TGGAGTCAGCATTTGGGAAC
GAPDH	F: TCAACGGCACAGTCAAGG
	R: TGAGCCCTTCCACGATG

SYP, synaptophysin; F, forward; R, reverse.

Results

Morphological changes in the nasal mucosa and adrenal gland in an OVA-induced allergic rhinitis mouse model. Sensitization of OVA in AR mice resulted in histopathological changes such as disordered arrangement of epithelial cells and cilia, inflammatory cells infiltration (lymphocytes and eosinophils) and interstitial swelling, compared with control mice (Fig. 2A). The expression of NGF and TrkA proteins in the AR mice nasal mucosa tissues increased significantly compared with control mice (Fig. 2B and C). As expected, OVA-sensitized mice developed increased sneezing and nasal rubbing compared with the control mice (Fig. 2D). TEM analyses revealed a regular arrangement of the cortical and medulla cells of adrenal glands in the control group: Medulla cells were characterized by clear mitochondrial structures, uniform distributions of chromaffin particles, round nuclei and smooth nuclear membranes. In the AR model group, there were changes in the apoptosis levels of AMCCs, manifested as nuclear membrane shrinkage, loose particle distribution and disintegration of cell contents. The AMCCs in the NGF group were characterized by swelling of cytoplasm, edema of mitochondria and protrusions. However, widened intercellular spaces and decreased mitochondrial swelling in AMCCs of K252a group were observed by TEM (Fig. 2E).

Endocrine functional changes of adrenal medulla from mice with the intervention of NGF. From Fig. 2, it was found that immunostaining of PNMT was mainly expressed in the adrenal cytoplasm. The expression levels of PNMT were much weaker in model and NGF groups compared with the control group. However, K252a treatment could promote the expression level of PNMT (Fig. 3A). To explore whether SYP is associated with the pathogenesis of AR, the expression levels of SYP mRNA and protein were detected by RT-qPCR and western blotting, respectively. Compared with the control group, significantly increased SYP mRNA and protein were found in the model and NGF groups. In addition, the NGF

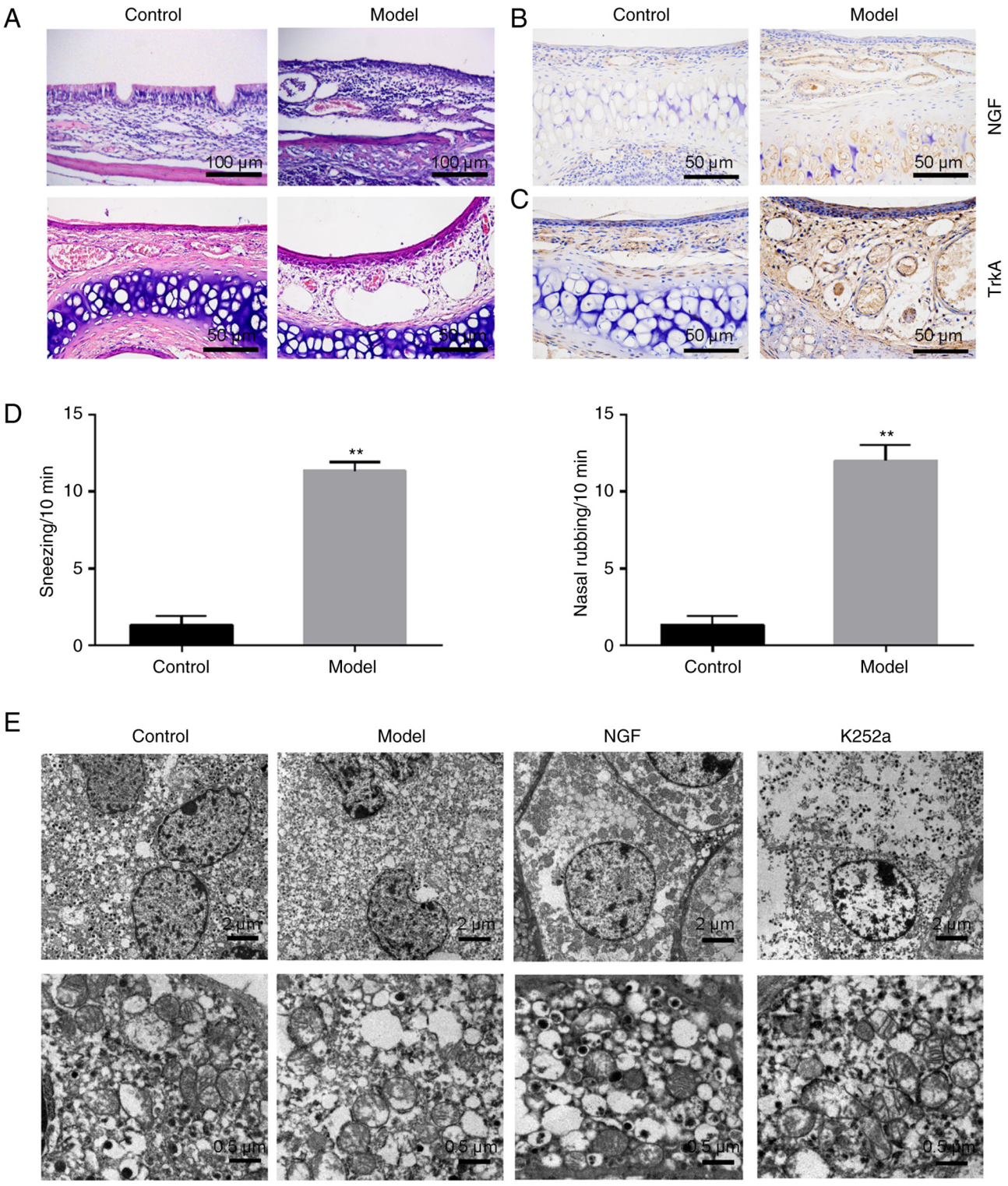

Figure 2. Pathological changes in the nasal mucosa and adrenal medulla tissues in the allergic rhinitis mouse model. (A) Hematoxylin and eosin-stained nasal mucosa tissue sections from mice. Representative micrographs of nasal mucosa tissues from control and model groups. Scale bars, 50 μm (above), 100 μm (below). (B) The representative sample of NGF immunostaining (DAB) was presented for the control and model groups. Scale bars, 50 μm. (C) A representative sample of TrkA immunostaining (DAB) was presented for the control and model groups. Scale bars, 50 μm. (D) Observation of the number of sneezing and nasal rubbing in mice following intranasal challenge. (E) TEM-captured morphological changes in the control group, model group, NGF group and K252a group. Scale bars, 2 μm (above) and 0.5 μm (below). **P<0.01 vs. control group. NGF, nerve growth factor; Trk, tropomyosin receptor kinase; TEM, transmission electron microscope.

group had even stronger expressions of both the SYP mRNA and protein than that in the model group, while the mRNA and protein levels of SYP were inhibited using the K252a (Fig. 3B and C).

The levels change of EPI and NE in serum of each group. The results showed that EPI secretions from serum were decreased in the model and NGF groups compared with control group, but this trend was inhibited with treatment K252a (Fig. 3D).

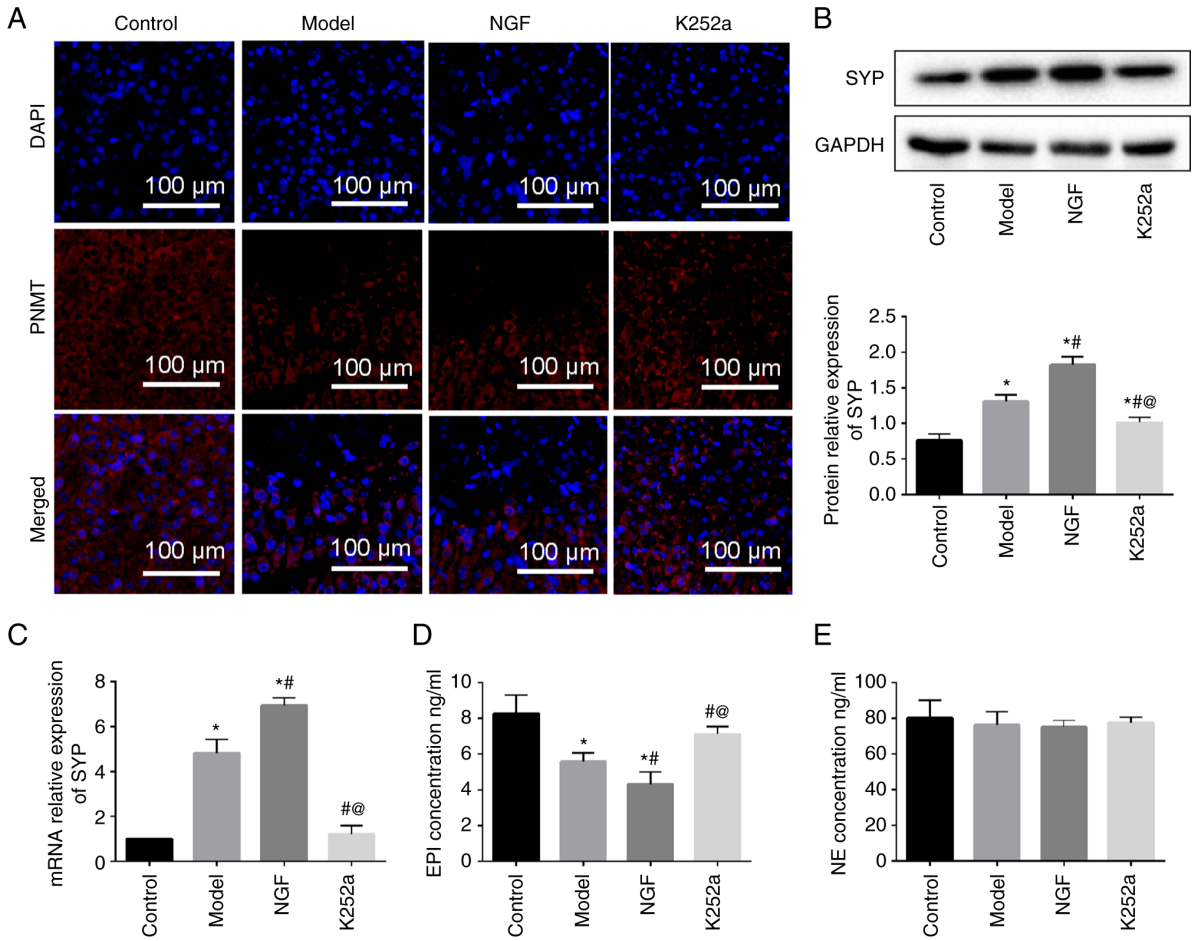

Figure 3. NGF-induced changes in the expression levels of PNMT and SYP in the adrenal medulla of mice with allergic rhinitis. (A) The change expression of PNMT (red) in adrenal medulla was detected by immunofluorescence. The nuclei of adrenal medulla were stained with DAPI stain (blue). Scale bars, 100 μm. (B) The protein and (C) total RNA were isolated from adrenal medulla and the expression of SYP (protein and mRNA) in each group detected by western blotting and reverse-transcription-quantitative PCR, respectively. ELISA-determined mice serum (D) EPI and (E) NE contents. *P<0.05 vs. control group, #P<0.05 vs. model group, @P<0.05 vs. NGF treatment group. NGF, nerve growth factor; PNMT, phenylethanolamine N-methyl transferase; SYP, synaptophysin; EPI, epinephrine; NE, norepinephrine.

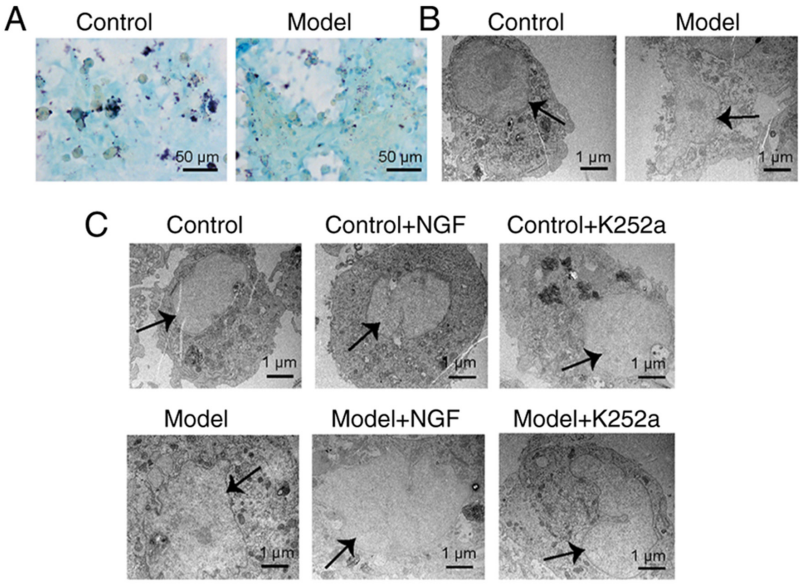

Figure 4. Identification of AMCCs and morphological changes in AMCCs following NGF treatment. (A) Giemsa staining and (B) TEM-identified isolated primary AMCCs (arrows indicate the nucleus). Scale bars, 50 μm (left), 1 μm (right). (C) The TEM-captured effect of NGF on the morphology of AMCCs (arrows indicate the nucleus). Scale bars, 1 μm. NGF, nerve growth factor; AMCCs, adrenal medulla chromaffin cells; NGF, nerve growth factor; TEM, transmission electron microscope.

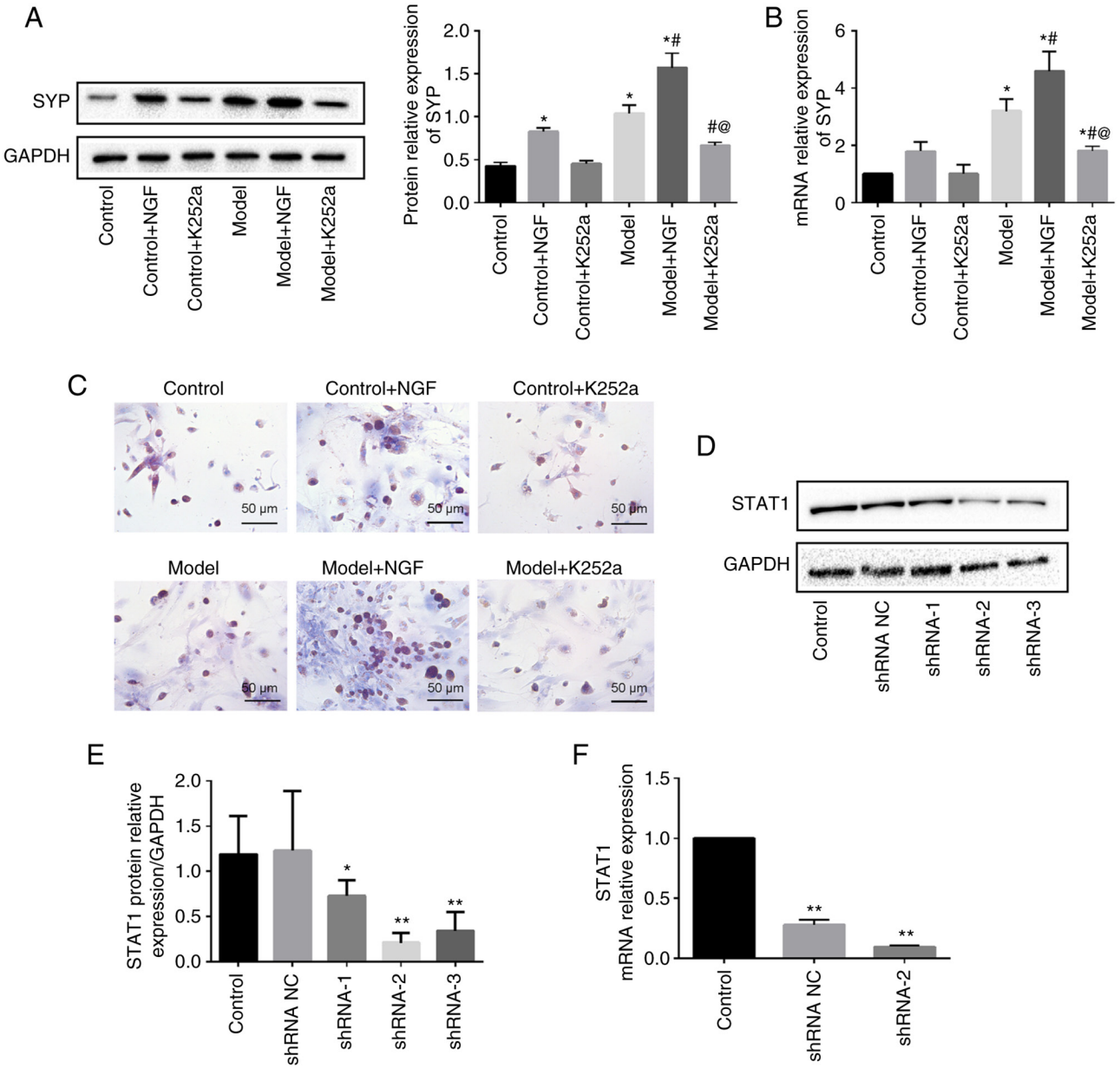

Figure 5. Changes in SYP expression in AMCCs treated with NGF. (A) Western blotting and (B) reverse-transcription-quantitative PCR-determined protein and mRNA expression changes in SYP in AMCCs. (C) Immunohistochemistry staining with a SYP antibody. Scale bars, 50 μm. (D and E) Western blot and (F) RT-qPCR-determined transfection efficiency of STAT1 shRNA in AMCCs. *P<0.05 and **P<0.01 vs. the control group, $^{\#}$P<0.05 vs. the model group, $^{@}$P<0.05 vs. the model + NGF group. SYP, synaptophysin; AMCCs, adrenal medulla chromaffin cells; NGF, nerve growth factor; sh, short hairpin.

However, there was no significant change in NE concentration in serum of mice in each group following intervention. (Fig. 3E). These results indicated that the endocrine function of adrenal medulla of mice changed following exogenous factors treatment, leading to the disorder of EPI secretion.

Identification of AMCCs and NGF-mediated morphological changes in AMCCs. Giemsa staining revealed that primary AMCCs isolated from the control and model groups had characteristically pale yellow cytoplasmic chromaffin granules (Fig. 4A). In addition, adrenal medulla cytoplasm harbored a uniform distribution of light black chromaffin cell secretory granules under TEM (Fig. 4B). Therefore, the isolated primary cells were possibly AMCCs. The AMCCs in the control group had intact morphologies and normal mitochondrial structures; however, AMCCs in the model group featured damaged nuclear structures, enlarged mitochondria and disintegrated contents (Fig. 4C). The AMCCs in the NGF + model group were more damaged compared with those in the model group, showing shrinkage of the nuclear membranes and further disintegration of contents. Treatment with K252a resulted in abundant villiform protrusions on cell membrane surfaces, the appearance of normal mitochondrial structures in the cytoplasm and the formation of small vesicles near cell membranes (Fig. 4C).

The effect of NGF and K252a on the biological behavior of AMCCs. The assessment of whether NGF affected the expression of SYP in AMCCs culminated in significantly increased SYP mRNA and protein levels when AMCCs were

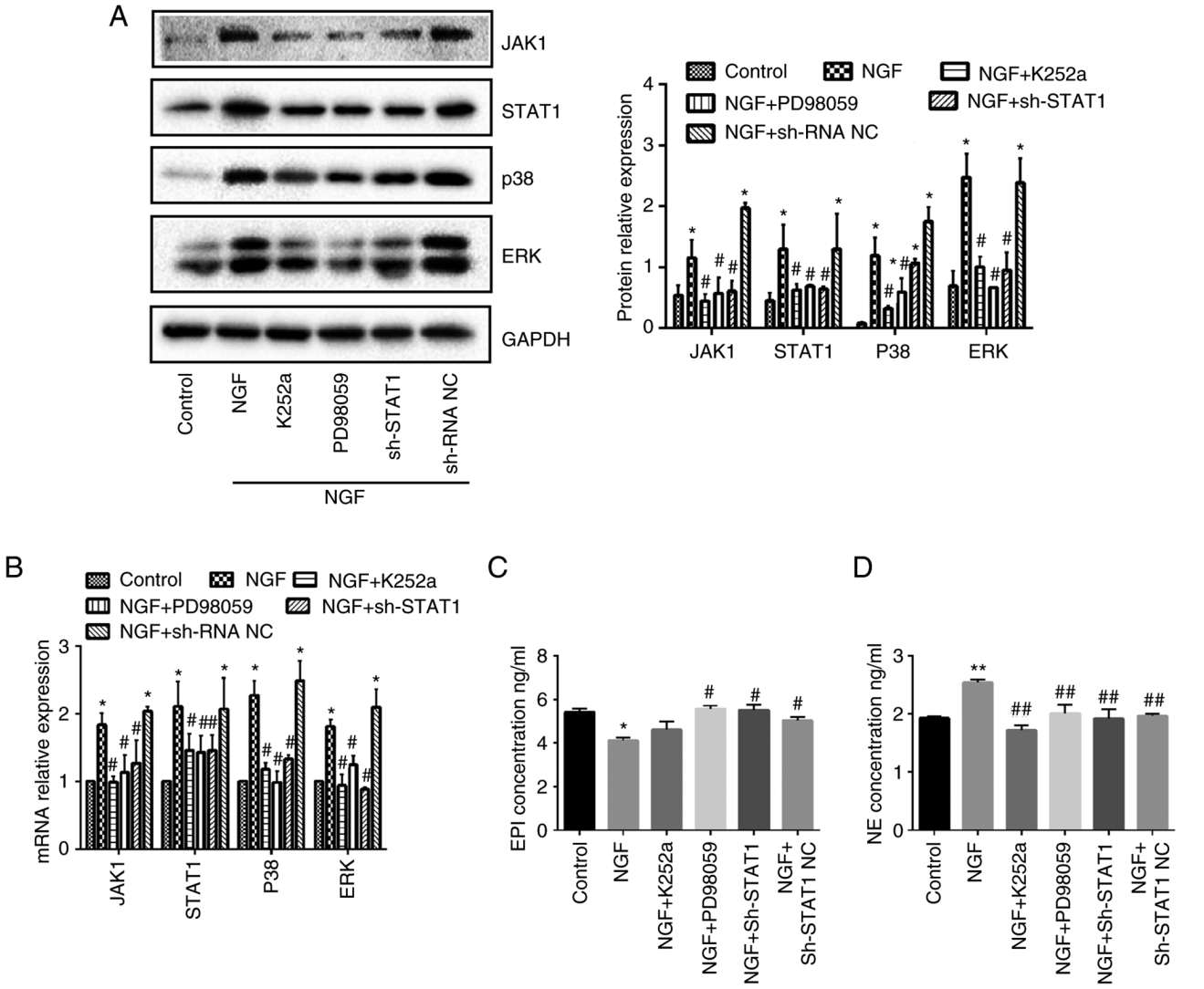

Figure 6. NGF-induces changes in the function and phenotype of AMCCs. (A) Protein and (B) mRNA levels of JAK1, STAT1, p38 and ERK in AMCCs treated under different conditions. ELISA-determined changes in the expression of (C) EPI and (D) NE. *P<0.05 and **P<0.01 vs. the control group, $^{\#}$P<0.05 and $^{\#\#}$P<0.01 vs. the model group. NGF, nerve growth factor; AMCCs, adrenal medulla chromaffin cells; EPI, epinephrine; NE, norepinephrine.

treated with NGF (Fig. 5A and B). In the presence of K252a, the mRNA and protein levels of SYP markedly decreased in AMCCs. Immunostaining localized SYP to the cytoplasm of AMCCs. The expression of immunostained SYP was enhanced in the presence of NGF, but K252a suppressed this expression (Fig. 5C). In summary, NGF participated in the alterations in the biological behavior of AMCCs.

The JAK1/STAT1, p38 and ERK pathways are substantially activated in AMCCs in the presence of NGF. STAT1 was knocked down with three pairs of designed shRNAs and selected the shRNA2 with the highest interference efficiency (Fig. 5D-F). NGF treatment significantly promoted the protein and mRNA expression levels of JAK1, STAT1, p38 and ERK in AMCCs compared with the control group. However, in the presence of K252a, PD98059 (the inhibitor of ERK) and STAT1 shRNA, the opposite observations were made. (Fig. 6A and B). These findings suggest that blocking NGF, ERK and STAT1 inhibited NGF-triggered signaling events in AMCCs.

EPI and NE concentrations change in cell supernatants treated with NGF. Compared with the control group, NGF presence resulted in diminished EPI concentrations and amplified NE levels in the supernatants of AMCCs. However, K252a, PD98059 and STAT1 shRNA treatments reversed this trend, increasing EPI expression and decreasing the levels of NE (Fig. 6C and D).

Discussion

The nasal mucosa, which is the first line of defense against allergen exposure, has an important role in maintaining the normal physiological function of the upper respiratory tract (31,32). Past investigations have pointed out that AR involves the infiltration of inflammatory cells, such as lymphocytes, eosinophils and basophils, into the nasal mucosa (33,34). The present study confirmed that lymphocytes and eosinophils infiltrated the nasal mucosa of AR mice, but not the control group. Additionally, the AR mice were characterized by increased nasal scratching and sneezing. Thus, an

OVA-induced mouse model of allergic rhinitis was successfully established.

Adrenal glands are crucial to maintaining the pathophysiological processes of an organism via the control of the endocrine system involved mainly in regulating hormone synthesis and responding to stress (35). The adrenal medulla is formed mostly by adrenergic and noradrenergic chromaffin cells. Histologically, both the chromaffin cells of the adrenal medulla and the sympathetic nerves of the autonomic nervous system originate from the neural crest of the ectoderm (36). Therefore, in addition to endocrine functions, chromaffin cells can also potentially transform into neuronal phenotypes. One previous investigation suggested that both mature and immature adrenal medulla cells possess varying degrees of pluripotent differentiation capacity (37). NGF, a member of the neurotrophin family, is critical in promoting the differentiation of cells (7). Stimulated by NGF, chromaffin cells can transform into neuronal phenotypes, with their original endocrine function also occurring with corresponding changes (27,37). In the present study, *in vivo*, lesions of the adrenal medulla were also accompanied by an AR onset and featured nucleolemma shrinkage, loose particle distribution and disintegration of cell contents under TEM. Notably, the present study revealed that treatment with NGF further aggravated adrenal medulla lesions *in vitro*; however, the degree of adrenal medulla lesions was alleviated by K252a. As an inhibitor of NGF receptor, K252a inhibits the activation of NGF-induced signaling pathway and downstream signals. A previous study reported that NGF could induce the transformation of microglial cells to a neuroprotective and anti-inflammatory phenotype, while K252a reversed this phenotypic transformation (38). K252a promotes the apoptosis of endometrial cancer cells, but it has little effect on normal human endometrial epithelial cells (39). As expected, K252a had no adverse effect on AMCCs. By contrast, it could antagonize the adverse effects of NGF on AMCCs. Together, when stimulated by NGF, ultrastructural changes (including mitochondrial swelling and nucleolemma shrinkage) occurred in the AMCCs of the AR mouse model and are possible evidence of cell phenotype switching.

SYP, which is a transmembrane protein of synaptic vesicles, is involved in the formation and circulation of synaptic vesicles (40,41). Additionally, SYP is a specific marker of neuroendocrine differentiation and is largely distributed in multiple organs, including the neurons, spinal cord and adrenal medulla (42). The present study found that NGF mediation resulted in notable augmentations in the SYP mRNA and protein levels *in vitro*; however, K252a reversed these trends. The results of immunohistochemistry further confirmed that the expression of SYP in the AMCCs of the AR model group and NGF intervention group was higher compared with that in the control group. Together, NGF presence induced an increase in the number of synapses in AMCCs to promote neuronal differentiation, while K252a inhibits this reaction.

PNMT is an enzyme biosynthesized by the adrenal medulla, which catalyzes the biosynthesis of catecholamines and methylates NE to form EPI (43). Since the final step in catalyzing EPI synthesis is PNMT, the changes in its expression levels indirectly reflect the number of EPI secretion. The endocrine function of AMCCs could be indirectly assessed using the level of PNMT (21). In the present study, it was

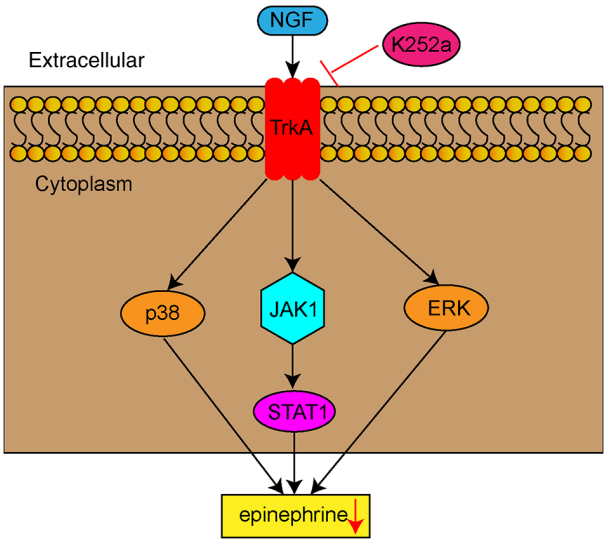

Figure 7. Schematic representation of NGF affecting the phenotypic differentiation of AMCCs. NGF induces the transformation of AMCCs from an endocrine phenotype to a neuronal phenotype through JAK1/STAT1, p38 and ERK signaling pathways, resulting in decreased epinephrine release. NGF, nerve growth factor; AMCCs, adrenal medulla chromaffin cells.

observed that the levels of PNMT in adrenal gland were downregulated in NGF and model groups, especially the NGF group. These results showed that reduced expression of PNMT by NGF stimulation might result in decreased EPI production. Therefore, the present study confirmed the changes in secretion of EPI *in vivo* and *in vitro* by ELISA. Compared with the control group, the serum levels of EPI were weakened in the model and NGF groups. However, the opposite trend was observed following K252a intervention. Decreased secretion of EPI in supernatants was observed when AMCCs were co-cultured with NGF. Some AMCCs possibly transform from endocrine phenotypes to neuronal cell phenotypes, accompanied by a decline in endocrine function, resulting in decreased synthesis and release of EPI in adrenal medulla cells. Chromaffin cells can differentiate into sympathetic neurons under NGF stimulation (26). Markedly, sympathetic neurons cannot synthesize and secrete EPI, but they produce and secrete NE (44). Furthermore, it was hypothesized that the increased levels of NE in cell supernatants arguably stemmed from the direct impact of NGF on AMCCs *in vitro*, resulting in the transformation of most chromaffin cells into sympathetic neuronal cells, widening the production of NE.

However, the signaling pathway through which NGF regulates the transdifferentiation of AMCCs remains to be elucidated. The ERK signaling pathway possibly participates in NGF-mediated neurite outgrowth in adrenal chromaffin cells (45). Neurotrophins including NGF and brain-derived neurotrophic factor (BDNF) regulate neuronal differentiation, survival and growth by binding to members of the Trk family, namely TrkA, TrkB and TrkC (46). A recent study showed that activation of BDNF/TrkB signaling pathway can lead to transactivation of several downstream signaling pathways, including PI3K/Akt, JAK/STAT, PLCγ, Ras-Raf-MEK-ERK and NF-κB (47). Activation of TrkA by NGF triggered phosphorylation of STAT3 at S727 and enhanced its DNA binding and transcriptional activity. TrkA-induced STAT3 activation

mediated several downstream functions of NGF signaling, particularly neuronal differentiation (48). The present study showed that NGF stimulation was linked to significantly enhanced protein and mRNA levels of JAK1, STAT1, p38 and ERK in AMCCs; however, K252a, PD98058 and STAT1 shRNA markedly suppressed the activation of these pathways. Therefore, NGF induced the conversion of AMCCs to a neuronal phenotype by activating JAK1/STAT1, p38 and ERK signaling pathways, resulting in epinephrine release dysfunction (Fig. 7). The present study was limited by the lack of analysis of their downstream signaling pathways. Whether the activation of these signaling pathways will be enhanced with the higher concentration of NGF is one focus of future research.

In summary, the present study suggested that NGF possibly affects the differentiation of AMCCs phenotypes in two main ways. First, sufficient amounts of NGF directly act on chromaffin cells to differentiate between endocrine phenotypes and sympathetic neuronal phenotypes. Second, increased NGF levels continuously act on chromaffin cells at different differentiation stages, gradually reducing their redundancy threshold, paving the way to eventually breaking through the anti-redundancy effect of glucocorticoids and transforming into sympathetic neuronal phenotypes. Hence, the mechanism of the transformation of AR into BA in a mouse model could be as follows: the increased concentration of NGF in AR mice directly affects the differentiation of chromaffin cells and then transforms them from an endocrine phenotype to a neuronal phenotype, thereby inhibiting EPI synthesis and release them into AMCCs, making it difficult to reach the concentration of diastolic airways to induce BA.

Overall, the present study demonstrated the effect of NGF on AMCCs *in vitro* and *vivo* and elucidated the pathogenesis of AR's transformation into BA and the correlation between the two airway diseases. Therefore, it could provide new theoretical support for the theory of 'one airway, one disease' (49).

Acknowledgements

Not applicable.

Funding

The present study was supported by the Natural Science Foundation of China (grant nos. 81460004 and 82160006); the Jiangxi Provincial Cultivation Program for Academic and Technical Leaders of Major Subjects (grant no. 20172BCB22025); and the Jiangxi Provincial Natural Science Foundation General Project (grant no. 20202BAB206003).

Availability of data and materials

The datasets used and/or analyzed during the current study are available from the corresponding author on reasonable request.

Authors' contributions

JW and CL conceived and designed the present study. XH, ZL, ZW, ND and AZ performed the experiments. JL and XH analyzed the experimental data. CL and JL wrote the manuscript. CL and JW confirm the authenticity of all the raw data. All authors have read and approved the final manuscript.

Ethics approval and consent to participate

The present study was approved by the Animal Care and Committee of Jiangxi Provincial People's Hospital (approval no. 2022-008; Nanchang, China).

Patient consent for publication

Not applicable.

Competing interests

The authors declare that they have no competing interests.

References

1. Testa D, DI Bari M, Nunziata M, Cristofaro G, Massaro G, Marcuccio G and Motta G: Allergic rhinitis and asthma assessment of risk factors in pediatric patients: A systematic review. Int J Pediatr Otorhinolaryngol 129: 109759, 2020.
2. Corren J: The connection between allergic rhinitis and bronchial asthma. Curr Opin Pulm Med 13: 13-18, 2007.
3. Zhang Y, Lan F and Zhang L: Advances and highlights in allergic rhinitis. Allergy 76: 3383-3389, 2021.
4. Chen M, Wu Y, Yuan S, Tang M, Zhang L, Chen J, Li L, Wu J, Zhang J and Yin Y: Allergic rhinitis improvement in asthmatic children after using acaricidal bait: A randomized, double-blind, cross-placebo study. Front Pediatr 9: 709139, 2021.
5. Nappi E, Paoletti G, Malvezzi L, Ferri S, Racca F, Messina MR, Puggioni F, Heffler E and Canonica GW: Comorbid allergic rhinitis and asthma: Important clinical considerations. Expert Rev Clin Immunol 18: 747-758, 2022.
6. Ceci FM, Ferraguti G, Petrella C, Greco A, Tirassa P, Iannitelli A, Ralli M, Vitali M, Ceccanti M, Chaldakov GN, *et al*: Nerve growth factor, stress and diseases. Curr Med Chem 28: 2943-2959, 2021.
7. Freund-Michel V and Frossard N: The nerve growth factor and its receptors in airway inflammatory diseases. Pharmacol Ther 117: 52-76, 2008.
8. Rocco ML, Soligo M, Manni L and Aloe L: Nerve growth factor: Early studies and recent clinical trials. Curr Neuropharmacol 16: 1455-1465, 2018.
9. Zhang N, Xu J, Jiang C and Lu S: Neuro-Immune regulation in inflammation and airway remodeling of allergic asthma. Front Immunol 13: 894047, 2022.
10. Chen PC, Hsieh MH, Kuo WS, Kao HF, Hsu CL and Wang JY: Water-Soluble chitosan inhibits nerve growth factor and attenuates allergic inflammation in mite allergen-induced allergic rhinitis. J Allergy Clin Immunol 140: 1146-1149.e8, 2017.
11. Bresciani M, Lalibertè F, Lalibertè MF, Gramiccioni C and Bonini S: Nerve growth factor localization in the nasal mucosa of patients with persistent allergic rhinitis. Allergy 64: 112-117, 2009.
12. Tu W, Chen X, Wu Q, Ying X, He R, Lou X, Yang G, Zhou K and Jiang S: Acupoint application inhibits nerve growth factor and attenuates allergic inflammation in allergic rhinitis model rats. J Inflamm (Lond) 17: 4, 2020.
13. Raap U, Fokkens W, Bruder M, Hoogsteden H, Kapp A and Braunstahl GJ: Modulation of neurotrophin and neurotrophin receptor expression in nasal mucosa after nasal allergen provocation in allergic rhinitis. Allergy 63: 468-475, 2008.
14. Sobkowiak P, Langwiński W, Nowakowska J, Wojsyk-Banaszak I, Szczepankiewicz D, Jenerowicz D, Wasilewska E, Bręborowicz A and Szczepankiewicz A: Neuroinflammatory gene expression pattern is similar between allergic rhinitis and atopic dermatitis but distinct from atopic asthma. Biomed Res Int 2020: 7196981, 2020.
15. Coffey CS, Mulligan RM and Schlosser RJ: Mucosal expression of nerve growth factor and brain-derived neurotrophic factor in chronic rhinosinusitis. Am J Rhinol Allergy 23: 571-574, 2009.

16. Liu P, Li S and Tang L: Nerve growth factor: A potential therapeutic target for lung diseases. Int J Mol Sci 22: 9112, 2021.
17. Szczepankiewicz A, Rachel M, Sobkowiak P, Kycler Z, Wojsyk-Banaszak I, Schöneich N, Szczawińska-Popłonyk A and Bręborowicz A: Neurotrophin serum concentrations and polymorphisms of neurotrophins and their receptors in children with asthma. Respir Med 107: 30-36, 2013.
18. Ogawa H, Azuma M, Uehara H, Takahashi T, Nishioka Y, Sone S and Izumi K: Nerve growth factor derived from bronchial epithelium after chronic mite antigen exposure contributes to airway hyperresponsiveness by inducing hyperinnervation, and is inhibited by in vivo siRNA. Clin Exp Allergy 42: 460-470, 2012.
19. Hashimoto S: K-252a, a Potent protein kinase inhibitor, blocks nerve growth factor-induced neurite outgrowth and changes in the phosphorylation of proteins in PC12h cells. J Cell Biol 107: 1531-1539, 1988.
20. Terad K, Matsushima Y, Matsunaga K, Takata J, Karube Y, Ishige A and Chiba K: The kampo medicine yokukansan (YKS) enhances nerve growth factor (NGF)-induced neurite outgrowth in PC12 cells. Bosn J Basic Med Sci 18: 224-233, 2018.
21. Hu CP, Zou YQ, Feng JT and Li XZ: The effect of unilateral adrenalectomy on transformation of adrenal medullary chromaffin cells in vivo: A potential mechanism of asthma pathogenesis. PLoS One 7: e44586, 2012.
22. Furlan A, Dyachuk V, Kastriti ME, Calvo-Enrique L, Abdo H, Hadjab S, Chontorotzea T, Akkuratova N, Usoskin D, Kamenev D, *et al*: Multipotent peripheral glial cells generate neuroendocrine cells of the adrenal medulla. Science 357: eaal3753, 2017.
23. Feng JT and Hu CP: Dysfunction of releasing adrenaline in asthma by nerve growth factor. Med Hypotheses 65: 1043-1046, 2005.
24. Krakauer DC and Plotkin JB: Redundancy, antiredundancy, and the robustness of genomes. Proc Natl Acad Sci USA 99: 1405-1409, 2002.
25. Wu XM, Hu CP, Li XZ, Zou YQ, Zou JT, Li YY and Feng JT: Asthma pregnancy alters postnatal development of chromaffin cells in the rat adrenal medulla. PLoS One 6: e20337, 2011.
26. Unsicker K, Krisch B, Otten U and Thoenen H: Nerve growth factor-induced fiber outgrowth from isolated rat adrenal chromaffin cells: Impairment by glucocorticoids. Proc Natl Acad Sci USA 75: 3498-3502, 1978.
27. Li QG, Wu XR, Li XZ, Yu J, Xia Y, Wang AP and Wang J: Neural-Endocrine mechanisms of respiratory syncytial virus-associated asthma in a rat model. Genet Mol Res 11: 2780-2789, 2012.
28. National Research Council (US) Committee for the Update of the Guide for the Care and Use of Laboratory Animals: Guide for the Care and Use of Laboratory Animals. 8th edition. National Academies Press (US), Washington, DC, 2011.
29. Li HT, Chen ZG, Lin YS, Liu H, Ye J, Zou XL, Wang YH, Yang HL and Zhang TT: CpG-ODNs and budesonide act synergistically to improve allergic responses in combined allergic rhinitis and asthma syndrome induced by chronic exposure to ovalbumin by modulating the TSLP-DC-OX40L Axis. Inflammation 41: 1304-1320, 2018.
30. Livak KJ and Schmittgen TD: Analysis of relative gene expression data using real-time quantitative PCR and the 2(-Delta Delta C(T)) method. Methods 25: 402-408, 2001.
31. Bousquet J, Anto JM, Bachert C, Baiardini I, Bosnic-Anticevich S, Walter Canonica G, Melén E, Palomares O, Scadding GK, Togias A and Toppila-Salmi S: Allergic Rhinitis. Nat Rev Dis Primers 6: 95, 2020.
32. Nur Husna SM, Tan HT, Md Shukri N, Mohd Ashari NS and Wong KK: Nasal epithelial barrier integrity and tight junctions disruption in allergic rhinitis: Overview and pathogenic insights. Front Immunol 12: 663626, 2021.
33. Eifan AO and Durham SR: Pathogenesis of Rhinitis. Clin Exp Allergy 46: 1139-1151, 2016.
34. Meng Y, Wang C and Zhang L: Advances and novel developments in allergic rhinitis. Allergy 75: 3069-3076, 2020.
35. Haase M, Willenberg HS and Bornstein SR: Update on the corticomedullary interaction in the adrenal gland. Endocr Dev 20: 28-37, 2011.
36. Unsicker K, Huber K, Schütz G and Kalcheim C: The chromaffin cell and its development. Neurochem Res 30: 921-925, 2005.
37. Barreto-Estrada JL, Medina-Ortíz WE and García-Arrarás JE: The morphological and biochemical response of avian embryonic sympathoadrenal cells to nerve growth factor is developmentally regulated. Brain Res Dev Brain Res 144: 1-8, 2003.
38. Rizzi C, Tiberi A, Giustizieri M, Marrone MC, Gobbo F, Carucci NM, Meli G, Arisi I, D'Onofrio M, Marinelli S, *et al*: NGF steers microglia toward a neuroprotective phenotype. Glia 66: 1395-1416, 2018.
39. Takai N, Ueda T, Nishida M, Nasu K and Narahara H: K252a is highly effective in suppressing the growth of human endometrial cancer cells, but has little effect on normal human endometrial epithelial cells. Oncol Rep 19: 749-753, 2008.
40. Raja MK, Preobraschenski J, Del Olmo-Cabrera S, Martinez-Turrillas R, Jahn R, Perez-Otano I and Wesseling JF: Elevated synaptic vesicle release probability in synaptophysin/gyrin family quadruple knockouts. Elife 8: e40744, 2019.
41. Chang CW, Hsiao YT and Jackson MB: Synaptophysin regulates fusion pores and exocytosis mode in chromaffin cells. J Neurosci 41: 3563-3578, 2021.
42. Kasprzak A, Zabel M and Biczysko W: Selected markers (Chromogranin a, neuron-specific enolase, synaptophysin, protein gene product 9.5) in diagnosis and prognosis of neuroendocrine pulmonary tumours. Pol J Pathol 58: 23-33, 2007.
43. Sørensen DB, Johnsen PF, Bibby BM, Böttner A, Bornstein SR, Eisenhofer G, Pacak K and Hansen AK: PNMT transgenic mice have an aggressive phenotype. Horm Metab Res 37: 159-163, 2005.
44. Vega A, Luther JA, Birren SJ and Morales MA: Segregation of the classical transmitters norepinephrine and acetylcholine and the neuropeptide Y in sympathetic neurons: Modulation by ciliary neurotrophic factor or prolonged growth in culture. Dev Neurobiol 70: 913-928, 2010.
45. Mullenbrock S, Shah J and Cooper GM: Global expression analysis identified a preferentially nerve growth factor-induced transcriptional program regulated by sustained mitogen-activated protein kinase/extracellular signal-regulated kinase (ERK) and AP-1 protein activation during PC12 cell differentiation. J Biol Chem 286: 45131-45145, 2011.
46. Uren RT and Turnley AM: Regulation of Neurotrophin Receptor (Trk) signaling: Suppressor of cytokine signaling 2 (SOCS2) is a new player. Front Mol Neurosci 7: 39, 2014.
47. Malekan M, Nezamabadi SS, Samami E, Mohebalizadeh M, Saghazadeh A and Rezaei N: BDNF and its signaling in cancer. J Cancer Res Clin Oncol: Sep 29, 2022 (Epub ahead of print).
48. Miranda C, Fumagalli T, Anania MC, Vizioli MG, Pagliardini S, Pierotti MA and Greco A: Role of STAT3 in in vitro transformation triggered by TRK oncogenes. PLoS One 5: e9446, 2010.
49. Klain A, Indolfi C, Dinardo G, Licari A, Cardinale F, Caffarelli C, Manti S, Ricci G, Pingitore G, Tosca M, *et al*: United airway disease. Acta Biomed 92: e2021526, 2021.